

# IG-RL: Inductive Graph Reinforcement Learning for Massive-Scale Traffic Signal Control

Francois-Xavier Devailly, Denis Larocque, Laurent Charlin

**Abstract**—Scaling adaptive traffic-signal control involves dealing with combinatorial state and action spaces. Multi-agent reinforcement learning attempts to address this challenge by distributing control to specialized agents. However, specialization hinders generalization and transferability, and the computational graphs underlying neural-networks architectures—dominating in the multi-agent setting—do not offer the flexibility to handle an arbitrary number of entities which changes both between road networks, and over time as vehicles traverse the network. We introduce Inductive Graph Reinforcement Learning (IG-RL) based on graph-convolutional networks which adapts to the structure of any road network, to learn detailed representations of traffic-controllers and their surroundings. Our decentralized approach enables learning of a transferable-adaptive-traffic-signal-control policy. After being trained on an arbitrary set of road networks, our model can generalize to new road networks, traffic distributions, and traffic regimes, with no additional training and a constant number of parameters, enabling greater scalability compared to prior methods. Furthermore, our approach can exploit the granularity of available data by capturing the (dynamic) demand at both the lane and the vehicle levels. The proposed method is tested on both road networks and traffic settings never experienced during training. We compare IG-RL to multi-agent reinforcement learning and domain-specific baselines. In both synthetic road networks and in a larger experiment involving the control of the 3,971 traffic signals of Manhattan, we show that different instantiations of IG-RL outperform baselines.

**Index Terms**—Deep reinforcement learning, Transfer learning, Adaptive traffic signal control, Graph neural networks, Zero-shot transfer, Independent  $Q$ -learning

## I. INTRODUCTION

THE steady growth of the world’s population, combined with a lack of space in urban areas, leads to intractable road congestion, the social and environmental costs of which are well documented [1]. The adaptive control of traffic signal systems based on real-time traffic dynamics could play a key role in alleviating congestion. The framing of adaptive traffic signal control (ATSC) as a Markov decision process (MDP) and the use of reinforcement learning (RL) to solve it via experiencing the traffic system is a promising way to move beyond heuristic assumptions [2], [3].

Value-based methods like  $Q$ -Learning constitute a cornerstone of RL. In practice however, using a single centralized learner [4], [5] in an ATSC setting with numerous traffic signal controllers (TSCs), involves a combinatorial action

space [6]. Multi-agent reinforcement learning (MARL), where each agent controls a single traffic light is appealing, but training and scaling remain challenging [2], [7], [8], [9].

### A. Contribution

We introduce inductive graph reinforcement learning (IG-RL) which combines the inductive capabilities of graph-convolutional networks (GCNs) [10] with a new decentralized RL (DEC-RL) framework. In our independent  $Q$ -Learning (IQL) formulation multi-agent RL is replaced by a shared policy, learnt and applied in a decentralized fashion.

We define the topology of the computational graph of the GCN based on the current dynamic state of the road network (e.g., including the position of moving entities such as cars).

The GCN learns and exploits representations of a neighborhood of arbitrary order for every entity of the road network, in the form of node embeddings. TSCs’ node embeddings are used to evaluate action-values (i.e.,  $Q$ -values). The entire model is differentiable and we train it using backpropagation of the temporal difference error (TD error), following a standard Deep  $Q$ -Learning setting [11]. By having the computational graph adapt to the road network’s state, we are able, for the first time to the best of our knowledge, to:

- Train a ubiquitous policy which can adapt to new road networks, including topologies and traffic never experienced during training.
- Exploit the vehicular data at its finest granularity by representing every vehicle as a node and its corresponding vectorized representation (i.e., embedding). Current neural-network architectures used in RL-ATSC do not enable dealing with a changing number of inputs and state dimensionality. For this reason, in a traffic scenario where various types of entities such as cars and pedestrians enter, move inside of, and leave the network, these methods do not enable full granularity exploitation. They typically resort, upstream of learning, to aggregations at the lane-level (e.g., the number of vehicles approaching the intersection) [2], [12], [13] or queues lengths [2], [12], [13]. Alternatively, they fix the number of entities to be represented in detail. For instance, [2] represents the cumulative delay of the first vehicle.

To test our claims, we define a new evaluation setting in which RL-ATSC methods are tested on road networks which are never experienced during training. In particular, we design two experiments involving non-stationary traffic distributions and different road networks.

F-X. Devailly, D. Larocque, and L. Charlin are with the Department of Decision Sciences at HEC Montréal, Québec, Canada. E-mail: francois-xavier.devailly@hec.ca, denis.larocque@hec.ca, laurent.charlin@hec.ca. This work was partially funded by the Natural Sciences and Engineering Research Council (NSERC), Fonds de Recherche du Québec : Nature et Technologies (FRQNT), Samsung, and Fondation HEC Montréal.

The first experiment, on synthetic road networks, evaluates IG-RL’s performance against both learnt and domain-specific baselines. We compare a *specialist* instance of IG-RL trained on the road network used during evaluation to a *generalist* that is trained on a set of road-networks which does not include the target road-network. These instances are compared to assess generalizability, transferability, and compare their efficiency to specialization. In addition, we also compare two GCN architectures which respectively capture traffic demand at the vehicle and lane levels, to measure the flexibility of IG-RL in different data conditions, and its ability to exploit granularity.

In the second experiment, an IG-RL instance is transferred, with no additional training (i.e., zero-shot transfer), to the road network of Manhattan and its 3,971 TSCs. This evaluation constitutes, by far, the largest RL-ATSC experiment to date. This final transfer from small synthetic road networks to a large real-world network aims to demonstrate the scalability of learning an agnostic policy.

The code we developed to perform all experiments will be open sourced upon publication.

## B. Related Work

The main thread of research this contribution draws on is decentralized RL (DEC-RL). In RL-ATSC, decentralization and distribution of control via multi-agent RL (MARL) is a popular approach [2], [7], [8], [9]. However, current MARL approaches used for ATSC suffer from the following caveats:

- From the perspective of a given agent (e.g. controller), the evolving behaviors of other agents (e.g. controllers) in the global environment cause nonstationarity and instability during training [14] [15]. [2] include the recent policies of other agents as part of the state of every local agent which seems to help but does not yet solve the problem.
- Without parameter sharing, though more scalable than previous approaches, computational resources and time required to train MARL approaches grow with every additional signalized intersection as it requires the training of additional agents.
- The specialization of every agent on the particular environment experienced by its jurisdiction during training hinders generalization and transferability to new environments. Therefore, applying MARL on any new road network or after any modification to a road network already under RL control requires training from scratch while interacting with road users and pedestrians to gather experience.

MARL and RL-ATSC in general, have therefore never, to the best of our knowledge, addressed the control of more than 196 TSCs [12]. In our work, instead of using MARL, we approach DEC-RL as a set of similar decision processes which can be controlled by a single agent and show results on a network of 3,971 lights.

A second thread which we draw from is graph neural networks, which have been shown to provide richer spatio-temporal representations of the road network and facilitate co-ordination [12] [13]. Instead of studying coordination however, we focus on leveraging the flexibility provided by graph neural

networks. [12] is concurrent work which also uses parameter sharing with graph neural networks. However, we propose both the use of transfer learning to provide further scalability, and a different method of encoding the dynamic road networks which enables exploiting granularity.

## II. BACKGROUND

### A. Reinforcement Learning (RL)

The optimization of a decision process under uncertainty can be framed as an MDP. An MDP is defined by a set of states  $S$ , a set of actions  $A$  that the agent can take, a transition function  $\mathcal{T}$  defining the probabilities of transitioning to any state  $s'$  given a current state  $s$  and an action  $a$  taken from  $s$ , and a reward function  $R$  mapping a transition (i.e.,  $s, a$ , and  $s'$ ) to a corresponding reward. Optimizing such a decision process means finding a policy  $\pi$ —a policy is a mapping from a state to the probability of taking an action—which maximizes the sum of the future rewards discounted by a temporal factor  $\gamma$ :

$$R_t = \sum_{k=0}^{\infty} \gamma^k r_{t+k+1} \quad (1)$$

where  $r_t$  represents the reward at timestep  $t$ . Reinforcement learning (RL) can be used to solve an MDP whose transition and value dynamics are unknown, by learning from experience gathered via interaction with the corresponding environment [16]. Off-policy RL refers to RL algorithms which enable learning from observed transitions regardless of the policy used to obtain them, by opposition to on-policy RL which can only use transitions obtained using the current behaviour derived from the learner. Since off-policy RL enables using any observation an arbitrary number of times, it is typically more sample efficient [17].  $Q$ -Learning is one of the most popular off-policy RL algorithm [18].

1)  $Q$ -Learning: The state-action-value function ( $Q$ -function) under policy  $\pi$  is the expected value of the sum of the discounted future rewards, starting in state  $s$ , taking action  $a$ , and then following policy  $\pi$ :

$$Q^\pi(s, a) = \mathbb{E}_\pi \left[ \sum_{k=0}^{\infty} \gamma^k r_{t+k+1} \mid s_t = s, a_t = a \right]. \quad (2)$$

From the optimal  $Q$ -function  $Q^* = \max_\pi Q^\pi$ , we can derive the optimal greedy-policy  $\pi^*(a|s) : a = \operatorname{argmax}_{a'} Q^*(s, a')$ .  $Q^*$  can be obtained by solving the Bellman equation [19]:

$$Q(s, a) = r(s, a) + \gamma \sum_{s' \in S} \mathcal{T}(s' | s, a) \max_{a' \in A} Q(s', a') \quad (3)$$

where  $r(s, a)$  is the immediate reward received after taking action  $a$  from state  $s$ .  $Q$ -Learning uses transitions sampled from the environment and dynamic programming to solve the Bellman equation with no initial knowledge of transition and reward functions. There are a few standard heuristics which enable  $Q$ -learning to model environments with large discrete or continuous state spaces. One of them consists in fitting the  $Q$ -function using buffers of experienced transitions which are large enough to prevent excessive correlations between

observed transitions. In continuous state spaces, tabular  $Q$ -Learning is replaced by a parametric model  $Q_\theta$  such as linear regression or a deep-neural network (DNN) [11]. In practice, the latter approach is referred to as Deep  $Q$ -Learning (DQL). Another heuristic consists in improving stability by keeping a lagging version of the model with recent parameters  $\theta^-$ , called target model  $Q_{\theta^-}$ , and using it to compute the temporal difference error (TD error):  $r(s, a) + \gamma \max_{a'} Q_{\theta^-}(s', a') - Q_\theta(s, a)$ . The TD error is backpropagated to update the parameters  $\theta$  following the corresponding  $Q$ -Learning update rule:

$$Q_\theta(s, a) \leftarrow Q_\theta(s, a) + \alpha \underbrace{\left[ r(s, a) + \gamma \max_{a' \in A} Q_{\theta^-}(s', a') - Q_\theta(s, a) \right]}_{\text{TD Error}} \quad (4)$$

where  $\alpha$  is the learning rate. Two standard extensions of  $Q$ -Learning led to promising results in our early RL-ATSC experimentation, and we use them in all our experiments:

- Double  $Q$ -Learning [20], which consists in reducing the overestimation of action values by decoupling action selection and action evaluation.
- Dueling  $Q$ -networks [21], which consists in enabling some parameters to focus on the relative advantage of actions by using additional parameters to evaluate the average of  $Q$ -values.

2) *Noisy Networks for Exploration*: Exploration via noisy networks refers to the use of parameterized noise, in the form of independent gaussian noise added to the parameters of a neural network, in order to favor consistent and state-dependent exploratory behavior [22]. In comparison to decaying  $\epsilon$ -greedy exploration—which consists in decaying the probability of acting randomly during training—noisy-network exploration often leads to better performances, enables online learning since it does not involve limiting exploration as time passes, and does not require tweaking sensitive learning schedules [22]. This form of exploration resulted in considerable improvements during our experiments and we use it to train all of models presented in this work.

3) *Decentralized Reinforcement Learning*: Decentralized reinforcement learning (DEC-RL) distributes the control based on the assumption that the global  $Q$ -function is decomposable [23]. IQL is a straightforward DEC-RL method in which the global MDP is decomposed into DEC-MDPs which are solved using independent  $Q$ -Learners.

## B. Graph Convolutional Networks

Enabling machine learning model to learn from complex relationships between objects in graphs is challenging. Graph Convolutional Networks (GCNs) are a recent and fruitful attempt to leverage neural-network architectures and back-propagation to address the complexity of graph data. GCNs consist in stacking  $k$  (a hyperparameter to be defined) convolutional layers as a neighborhood-information aggregation framework [24]. At every layer of a GCN, every node aggregates *communications* sent to it by both its neighbors and itself into an embedding. This form of embedding both exploits the

graph structure and the features of the nodes belonging to its neighborhood (up to order  $k$ ). Using different parameters for different types of relations [25] yields the following message propagation equation, applicable to every node:

$$n_i^{(l)} = f \left( \sum_{e \in E, j \in N_e(i)} C_{i,j,e} \cdot (W_{l_e} \cdot n_j^{(l-1)}) \right) \quad (5)$$

where  $n_i^l$  is the embedding of node  $i$  at layer  $l$ ,  $f$  is a non-linear differentiable function,  $E$  is the set of relation types,  $N_e(i)$  is the 1st-order neighborhood of node  $i$  in the graph of relation type  $e$ ,  $C_{i,j,e}$  is a relation-specific normalization constant, and  $W_{l_e}$  is the  $l^{\text{th}}$  layers weight matrix for message propagation corresponding to a relation of type  $e$ . Embeddings can be used to perform a supervised or unsupervised learning task, and an error signal corresponding to the task can be backpropagated through the entire model to perform gradient based optimisation of its parameters.

## III. INDUCTIVE GRAPH REINFORCEMENT LEARNING (IG-RL)

We now introduce IG-RL, a scalable DEC-RL method. IG-RL models objects (e.g., lanes, traffic signals, vehicles) as nodes in a graph. Edges of this (dynamic) graph represent the physical connections between objects (e.g., a vehicle node is connected to its current lane node).

A GCN models this graph. Initial node embeddings encode observable features of the objects (e.g. the vehicle speed). Each inferred TSC-node-embedding is used to predict the  $Q$ -values of that TSC.

The key for scaling and generalization is this graph representation. First, the GCN only instantiates a small number of parameters which are jointly learned across the entire road network. Second, once learned the GCN parameters are transferable to both new road networks and states (e.g., different traffic conditions) without additional learning.

### A. Decentralized ATSC Decision Processes

The state and action spaces of the global ATSC MDP, which consists in the management of all controllers in a given road network, can be large and intractable in practice. We therefore decompose it into smaller decentralized decision processes. In this context, the management of every intersection by a TSC becomes an MDP.

1) *State*: The state of every decentralized decision process consists in real-time information coming from local sensors and is said to be partially observable because it does not include all information about the global MDP. This state represents both current connectivity in the network, and demand. Connectivity of a given intersection is defined by the current phase of the corresponding TSC, while demand can be sensed either at the level of lanes, or at the level of vehicles.

2) *Action*: At every intersection of the road network, the flow of traffic is managed by a logical program, composed of a given number of phases, depending on the number of roads, the number of lanes, and the connectivity between lanes (see § III-B for details). This program cycles through phases, influencing connectivity between lanes, in a constant

predefined order that is often known to the road users and pedestrians. In our experimentations, the agent must respect the program and chooses, every second, whether to switch to the next phase or prolong the current phase. The action space at every intersection is therefore binary. Compared to methods which enable complete freedom of the controller, with the agent being able to choose among any phase every time it picks an action [2] [5], this formulation of the ATSC problem is more constrained. The agent must learn transition dynamics ruled by a complex cycle influencing connectivity. It is however more adaptive than methods determining duration upstream of any given phase [26]. We leave the exploration of other policy constraints for future work (in principle it is straightforward to adapt our method to different constraints).

3) *Reward*: The reward for a given agent is defined as the sum of local queues lengths  $q$ , which corresponds to the total number of vehicles stopped<sup>1</sup> on a lane leading to the corresponding intersection, at a maximum distance of 50 meters of the intersection. The reward at intersection  $j$  is

$$r_j = \sum_{i \in L_j} q_i \quad (6)$$

where  $L_j$  is the set of lanes leading to intersection  $j$ . This measure can both be obtained via lane or vehicular sensors. We choose this measure instead of alternatives such as wave [26] or average trip waiting time [7] because it is correlated to the local transition mechanisms of each DEC-MDP, and it is dense since actions tend to impact this measure quickly. These last two points translate into eased attribution of reward signals [2].

## B. Model

The control of all traffic signals form a family of decision processes. Each traffic-signal involves a controller, lanes, connections between lanes, and vehicles (e.g., nearby ones). A GCN is used to model these entities and their dynamic relationships. IG-RL proposes systematic sharing of the parameters of the GCN among all objects and relationships of the same nature. In addition, the flexibility of GCNs enables representing an arbitrary number of entities which changes over time (e.g., moving vehicles in the network) in a detailed way (i.e., as nodes).

1) *Architecture*: Figure 1 illustrates the GCN for modelling a traffic-signal control. It includes 4 types of nodes:

- *TSC node*, which represents the state of a controller.
- *Connection node*, which represents the state of an existing link between an entry lane and an exit lane. A link (i.e., connection node) exists between an entry lane A and an exit lane B if, under at least one phase of the TSC program, a vehicle on A is allowed to continue its travel on B.
- *Lane node*, which represents the state of a lane.
- *Vehicle node*, which represents the state of a vehicle.

The GCN uses the following edges and edge types:

- An edge between every node and itself (4 types of edges)

- Bidirectional edges between every *TSC node* and *Connection nodes* corresponding to connections the TSC can influence by changing its phase (2 types of edges)
- Bidirectional edges between every *Connection node* and *Lane nodes* corresponding to its entry lane (2 types of edges) and its exit lane (2 types of edges).
- Bidirectional edges between every *Lane node* and *Vehicle nodes* corresponding to vehicles located on the corresponding lane, given that the GCN exploits detailed vehicular data (2 types of links)

Every layer of the GCN uses one set of parameters per edge type to perform message-propagation. Our early experimentation with TSC suggested that using normalization constraints was detrimental to performance. In contrast to Equation 5, we do not include a normalization constraint during message-passing:

$$n_i^{(l)} = f\left(\sum_{e \in E, j \in N_e(i)} W_{l_e} \cdot n_j^{(l-1)}\right). \quad (7)$$

The embedding of a node  $j$  is initialized (i.e.,  $n_j^0$ ) using its features (see § III-B3). A fully connected layer, with a single set of parameters, maps the final node embedding of a TSC to the  $Q$ -values corresponding to its selectable actions.

Since preliminary experiments demonstrate that noisy exploration enables faster and more robust training, as well as better performance compared to  $\varepsilon$ -greedy exploration, parameterized gaussian noise is added to the parameters of this final mapping. An initialization of 0.017 for the variance parameters performs well in multiple supervised [22] and reinforcement learning tasks [27], and so we also use that value. Figure 1 is an illustration of the architecture of the full model for a simple road network with a single TSC and three vehicles.

2) *Parameter Sharing*: With the proposed architecture, parameters are shared both inside of a given decision process (e.g., between two lanes on a same intersection), and across all decision processes belonging to the corresponding family (e.g., between two lanes on unrelated intersections). We seek systematic parameter sharing for the following reasons:

- It enables sharing a constant number of parameters among an arbitrary number of decision processes with varying structures and complexities.
- It enables training these parameters on a variety of decision processes (e.g., on a training set of road-networks involving intersections of varying topologies). Such variety ensures the decorrelation of experiences during training. A diversified training set forces generalization of learnings and can therefore reduce over-fitting. In turn, forcing generalization in this manner can translate into more efficient transfer [28] [29]. In addition, we hypothesize that a diversified training set can limit non-stationarity in DEC-RL by marginalizing out the particular behaviours of a given controller's neighbors.

3) *Features*: Our approach exploits data that can be accessed from sensors representing the various entities that make up the road network and traffic. At any timestep in a given road network, every element defining the state is represented through a node in the GCN. The architecture of

<sup>1</sup>A vehicle is considered stopped if its speed is inferior to 0.1km/h

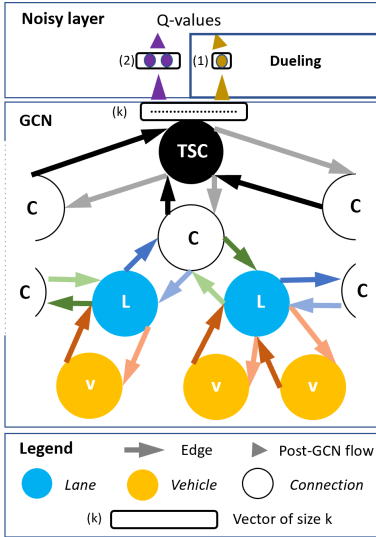


Fig. 1. Model. We illustrate the computational graph corresponding to one of the connections a TSC observes at its intersection. One vehicle is located on the connection’s inbound lane while two are located on its outbound lane. In this particular example, both lanes are only involved in a single connection on the intersection and respectively start from and lead to other intersections. For every layer of the GCN, message-passing is performed along every edge following Equation 7. Edges of the same type share the same color and parameters. The final embedding of the TSC node is then passed through the a fully connected layer to obtain its  $Q$ -values (one per possible action).

the GCN is built on the assumption that the current state of the controller (i.e., the current phase and its corresponding local connectivity) is known, and that traffic information coming either from lane sensors or vehicle sensors is also available. Other assumptions would result in the choice of a different GCN architecture or in the use of different features. The features used for different types of nodes are summarized in Table I. *Current speed* represents the current speed of a vehicle in km/h, *Position on lane* represents the relative location of a vehicle with respect to the lane it is on. It is defined as a proportion of the lanes length. *Length* is the length of a lane in meters, *Number of vehicles* is the total number of vehicles captured by the lanes sensor, *Average vehicles speed* is the average speed of vehicles captured by the lanes sensor, *Is open* represents whether a connection is opened under the current phase, *Has priority* represents whether, if an open connection between an entry and an exit lane has priority or not. *Number of switches to open* is the number of switches the controller has to perform before the next opening of a given connection. *Next open has priority* defines whether the next opening of the connection will have priority or not. *Time since last switch* is the number of seconds since a traffic controller performed its last phase switch.

#### IV. EXPERIMENTS

Using the SUMO traffic simulator [30] we evaluate the performance of several IG-RL instantiations using small synthetic-road networks and a large real-road network, and

<sup>1</sup>Vehicles may use a connection (i.e., go from its entry lane to its exit lane) if no vehicle uses a higher prioritised connection

TABLE I  
INITIAL STATE VARIABLES FOR EVERY TYPE OF NODE.

Type of node	State features
Vehicle	<i>Current speed, Position on lane</i>
Lane	<i>Length, Number of vehicles, Average vehicles speed</i>
Connection	<i>Is open, Has priority, Number of switches to open, Next opening has priority</i>
TSC	<i>Time since last switch</i>

compare it to the results of several baselines. Our study demonstrates that:

- IG-RL outperforms all included baselines on the ATSC task in a traditional evaluation setting.
- Training IG-RL under several varying initial conditions (including different road networks) yields the best performing method and enables zero-shot transfer.
- Training IG-RL on small synthetic road networks with limited computational resources enables efficient zero-shot transfer to real road networks, and such a transfer translates into improved scalability.

The process of designing a training set of synthetic examples (random road networks) before transferring the learnt policy to a more realistic setting (Manhattan) is inspired by other zero-shot transfer approaches in reinforcement learning [31] [32].

##### A. IG-RL models

1) *Architectures*: Our complete GCN architecture, referred to as IG-RL-Vehicle (IG-RL-V), uses a 3-layer GCN and vehicle-level traffic information for both state<sup>2</sup> and reward (§ III-A).

We also introduce a lighter GCN architecture, IG-RL-Lane (IG-RL-L) which uses a 2-layer GCN and lane-level traffic information for both state<sup>3</sup> and reward (§ III-A). Even though IG-RL-L does not exploit demand at the vehicle-level, it has the added benefit of requiring constant computational time with respect to the traffic demand.

For both IG-RL-L and IG-RL-V, the number of layers is chosen to be the minimum which ensures that information representing demand can reach the nearest TSC(s) nodes. For both GCN architectures, we use embedding of size 32 as further increasing it did not result in improved performances.

2) *General versus Specialized*: The target network refers to the road network used to test the performance of a method after training and must be distinguished from the training set of road-networks since the same IG-RL instance can be applied on different road networks. Two training sets of road-networks are built for IG-RL. The *generalist set*, used to train Generalist-IG-RL (G-IG-RL), aims to study its transfer abilities. It consists in training the model on a set of independent road networks which never includes the target road network. The intention behind training IG-RL on a variety of structures is to force the learning of patterns that generalize better and

<sup>2</sup>Lane level traffic features are not included in IG-RL-V.

<sup>3</sup>Vehicle nodes are not included in IG-RL-L.

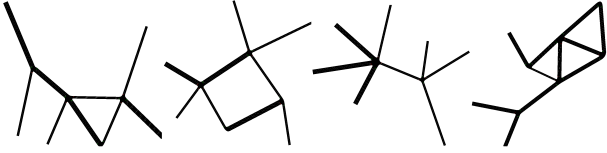


Fig. 2. Four randomly generated road networks. Thickness indicates the number of lanes per direction (between 1 and 2 per direction for a maximum of 4 lanes per edge).

improve zero-shot transfer to new networks. The *specialist set*, used to train Specialist-IG-RL (S-IG-RL), aims to evaluate whether intentional specialization on a given network is able to outperform G-IG-RL. It consists in training the model exclusively on the target road network. (Our experiments with hybrid training sets involving both the target road network and random road networks did not lead to improved performance compared to the generalist approach and are omitted for brevity.)

3) *Action Correction*: To evaluate the value of action correction (see § III-A2), we introduce a version of IG-RL-L for which no action correction is performed during training. This ablation study is referred to as IG-RL-no-correction (IG-RL-n-c).

## B. General Setup

1) *Network Generation*: The structure of a road network is picked, at random, from a set which consists in the cross product of the number of intersections (typically between 2 and 6), the structure of every intersection, the length of every edge (between 100 and 200 meters), the number of lanes per route (between 1 and 4 per edge), and general connectivity. A given random seed will lead to the generation of the same network, enabling exact comparison of performance between policies. Examples of randomly generated networks from our procedure are shown in Figure 2.

2) *Traffic Generation*: A given number of trips are to be generated per second, on average, during an episode. Every generated trip is assigned a trajectory. A trajectory is defined by a starting lane, a sequence of intermediary lanes, and a final lane. Every valid trajectory includes at least 2 lanes. To simulate the urban setting, a trajectory can start and end anywhere in the network. Parameters defining non-uniform distributions used for assigning trajectories to trips are re-sampled every 2-minutes to ensure non-stationary distributions.

3) *Training sets*: Models are trained on a set of 30 simulations running in parallel. During training, exploratory behaviors tends to lead to catastrophic congestion from which recovery becomes unlikely. This is a common RL challenge which makes training from long episodes inefficient in practice. For this reason, as in [2], every simulation runs 30,000 steps divided into independent short episodes of 500 steps (seconds) each. All simulations run on a single randomly generated road network. We also use this network for evaluation in our first experiment (§ IV-D). Further, each simulation is initialized using a different random seed to ensure a variety of observed transitions. Models are trained using the exact same environment (network and demand). The parameters of target

$Q$ -networks are updated every 100 parameters updates of the main  $Q$ -networks (§ II-A1) The learning rate is 0.001 and the batch size is 16.

Generalist: The generalist training set used to train G-IG-RL substitutes the target road network with 30 random road networks during training.

4) *Evaluation*: All methods are evaluated using the same target networks and identical demand. However, evaluation introduces traffic regimes (densities) never experienced during training. Recall that we introduce a new RL-ATSC evaluation setting for G-IG-RL. In this setting, while G-IG-RL is evaluated using the same network and the same demand that is used for other methods in order to be able to compare performances, it is trained on a set of independent networks which does not include the target network. In such a context, performance does not only reflect generalizability to new demand and new traffic regimes, but also generalizability to new road network and intersection architectures. We evaluate performance by measuring the evolution of instantaneous delay:

$$s_v^* = \min(s_{v^*}, s_l),$$

$$d_t = \sum_{v \in V} (s_v^* - s_v) / s_v^* \quad (8)$$

where  $V$  is the set of all vehicles in the road network,  $s_{v^*}$  is the maximum speed of the vehicle,  $s_l$  is the maximum allowed speed on the lane the vehicle is on,  $s_v$  is the current vehicle speed, and  $d_t$  is the total instantaneous delay at timestep  $t$ . Given that all models are evaluated on the same sets of networks and trips, we can study detailed trip-durations and pair the same trips, where traffic is controlled using different models, together to study distributions of paired differences.

5) *Constraints*: Phases involving yellow lights last 5 seconds, as suggested by [26]. For any other phase, in order to ensure true adaptiveness, instead of using a fixed time of 5 seconds between every action as suggested by [2], we let a TSC switch to the next phase at any chosen step (i.e., second), given that the last switch was performed at least 5 seconds ago.

Because of this constraint, in many situations, even though the agent can pick an action, this decision has no influence on the MDP. For instance, the agent might evaluate the action corresponding to a switch to the next phase as being optimal, but if the last switch is too recent, no change will be performed. This forces agent(s) to learn that the effect of the available actions on connectivity are dependent on other logical factors like the time since the last phase change and the nature of the current phase. To ease learning, and since it is preferable to focus on the actual influence an agent can have on its MDP, we replace, during experience replay, binary decisions which were chosen by the agent at every timestep, by whether a light switch was performed. We also force the greedy policy, in the creation of the temporal difference target, to only consider actions which could be performed at the corresponding step.

6) *Robustness*: The seeds we use in the experiment influence the random generation of road networks, traffic distributions, initial weights of neural networks, and the Gaussian noise used for exploration during training. To ensure the robustness of our conclusions, every experiment, including

both training and test, is repeated 5 times using different seeds. For instance, the training on 30 different simulations occurs 5 times for a total of 150 simulations. The same goes for evaluation. Reported test results are an aggregation over these 5 runs for both experiments.

### C. Baselines

We now describe the models used as baselines in both of our experiments.

1) *Fixed Time Baseline*: This baseline follows the cycle of phases using predefined and constant phases duration generated by SUMO [30] based on the architecture of each intersection.

2) *Max moving car heuristic*: This dynamic heuristic-based method aims at ensuring that as many vehicles as possible are moving on inbound lanes at any given time. At every intersection, the controller switches to the next phase if, on inbound lanes, the number of stopped vehicles is superior to the number of moving vehicles, and prolongs the current phase otherwise.

3) *MARL-IQL*: MARL-IQL is a learnt baseline. In this model, every intersection is controlled by its corresponding agent (i.e., with its own unique parameters), which learns to solve its own local MDP. Every agent, parameterized by a deep  $Q$ -Learner network, takes the exact same variables that are available to IG-RL-L as inputs (see Table I and § IV), with the exception of lanes *lengths*, which is constant for each MDP. Every  $Q$ -Learner consists of a first hidden layer of 256 neurons, a second hidden layer of 128 neurons and a last hidden layer of 64 neurons, which is the result of a grid-hyperparameter search. While this model would constitute a “vanilla” multi-agent implementation, we chose to add both Double  $Q$ -Learning and a Dueling architecture to every  $Q$ -Learner (see § II-A1) as done in [33]. In addition, the introduction of noisy parameters (see § II-A2) and action correction (see § IV-B5), were the elements which led the the biggest improvements during training. These improvements have the two following objectives:

- Create a strong baseline.
- Enable an ablation study. The only difference between MARL-IQL and S-IG-RL-L is that the former uses one neural network per intersection to learn the local  $Q$ -function and compute the local  $Q$ -values, while the latter uses the same GCN to do so at every intersection. Apart from this, all the information and methods they use for training are identical.

### D. Experiment 1: Transferability and Flexibility

1) *Description*: In this experiment, we evaluate and compare the performances of all methods on the road network which is also used to train all methods except G-IG-RL. MARL-IQL cannot scale as efficiently as IG-RL methods and so we picked a small road network and could train both families of methods on it.

This task remains challenging even if the road network is the same in training and evaluation. While methods are evaluated during episodes of more than an hour, they are trained on

shorter episodes of 500 seconds (see §IV-B3). During evaluation, trips are generated during the first hour, and simulation ends as soon as all trips are completed. Performance of all methods are evaluated using 30 different random seeds for traffic generation. Evaluation is run twice, with two distinct traffic regimes (denoted *default* and *heavy*), in order to evaluate the ability of models to generalize to traffic densities never experienced in training, as well as to study the performance in different density settings. The first evaluation traffic regime, which is the one used during training, introduces an expected one vehicle per second in the network, while the second traffic regime introduces twice as many per second in expectation.

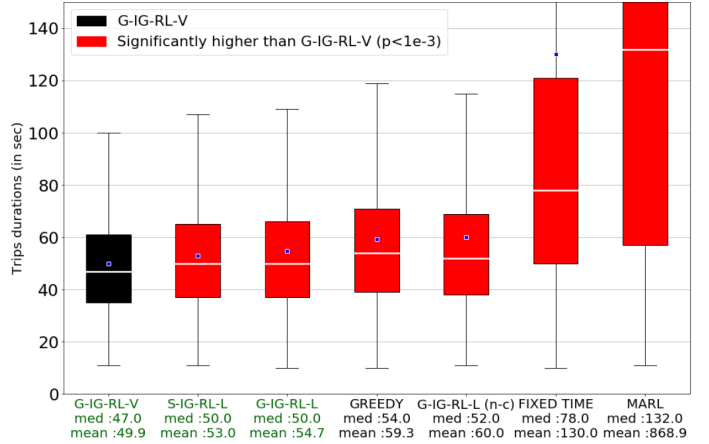


Fig. 3. Trips Durations: **Default** Traffic Regime — Synthetic Road Networks. This figure presents the distribution of trips durations during test on the same traffic regime which is used during training. The vertical axis is cut at MARL’s median trip duration for readability. Since every method is evaluated using the exact same trips, for every method, we perform t-tests on the paired sample of: 1) The durations of the trips when using the given method 2) The durations of the trips when using G-IG-RL-V. The results of these paired t-tests suggest that G-IG-RL-V significantly outperforms every other method, while the boxplots, means and medians of trips durations suggest that IG-RL models using action correction outperform all other methods in general.

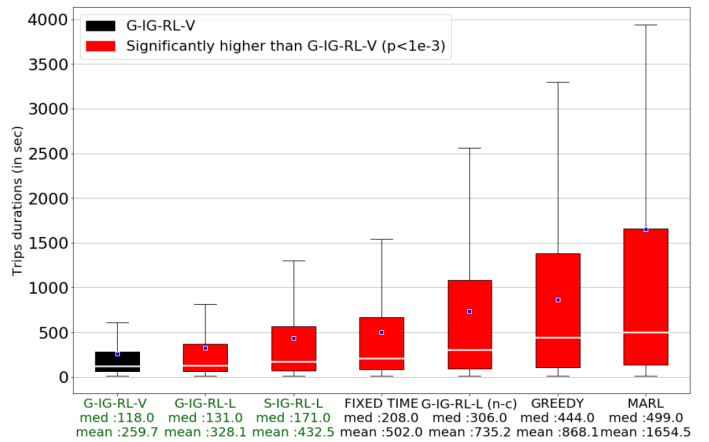


Fig. 4. Trips Duration: **Heavy** Traffic Regime — Synthetic Road Networks. This figure presents the distribution of trips durations during test using the heavier traffic regime that was not experienced during training. Results are again in favor of G-IG-RL-V and IG-RL methods in general. Performance gains are larger in this setting.

2) *Results*: We now refer to the group of methods using both IG-RL and action correction as IG-RL models, and highlight them in all following figures (green font). Additionally,

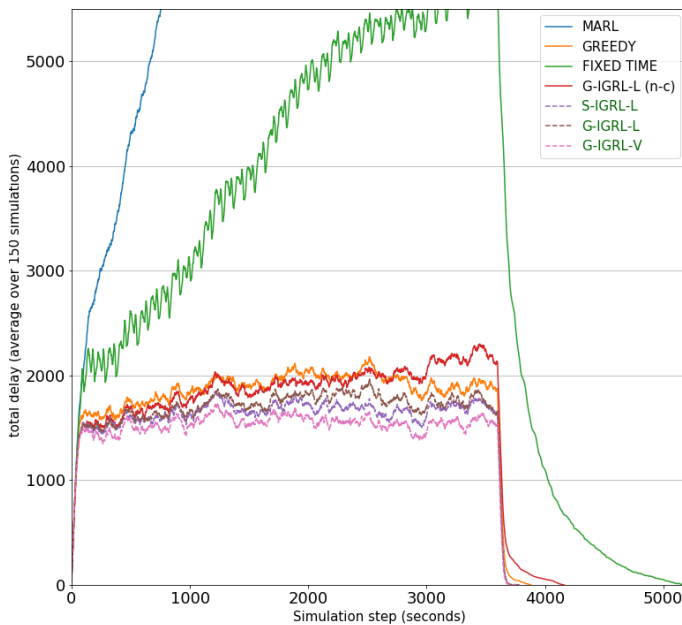


Fig. 5. Total Delay Evolution: **Default** Traffic Regime — Synthetic Road Networks

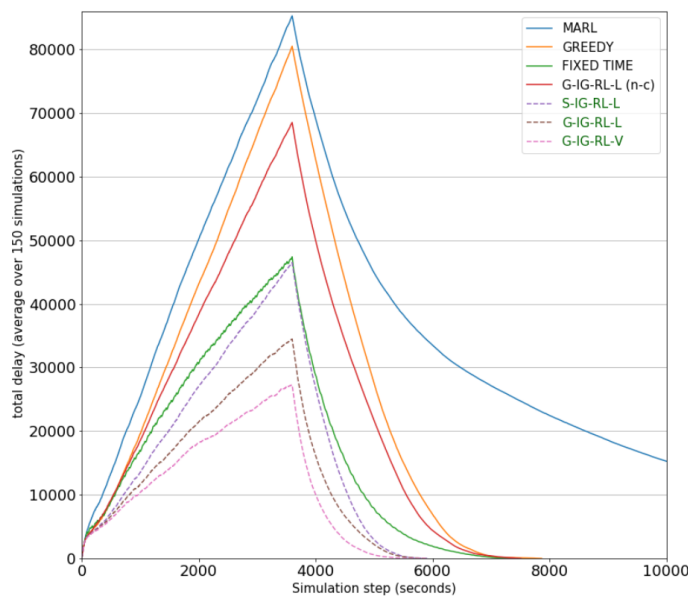


Fig. 6. Total Delay Evolution: **Heavy** Traffic Regime — Synthetic Road Networks

the max moving car heuristic baseline is referred to as *greedy* in all following figures. Means and medians of trip durations, reported in Figure 3 and Figure 4, are lower when using IG-RL models, compared to other methods. Instantaneous total delays, reported for every simulation step in Figures 5 and 6, show that congestion increase is slower, and recovery<sup>4</sup> is faster using IG-RL models on both traffic regimes. In addition, on the default traffic regime, these methods reach the lowest steady-state in terms of congestion level.

A key finding emerges from comparing G-IG-RL-L and S-

<sup>4</sup>Recovery refers to the speed at which delay decreases after the simulation reached 1 hour and no additional trips are generated.

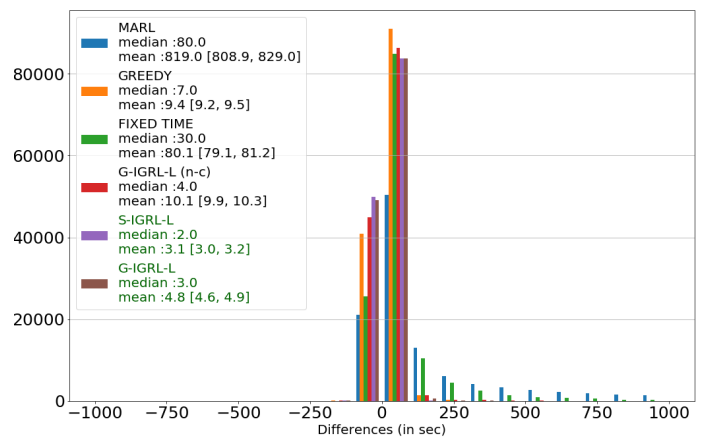


Fig. 7. Differences of Paired Trips Durations (compared to G-IG-RL-V) : **Default** Traffic Regime — Synthetic Road Networks

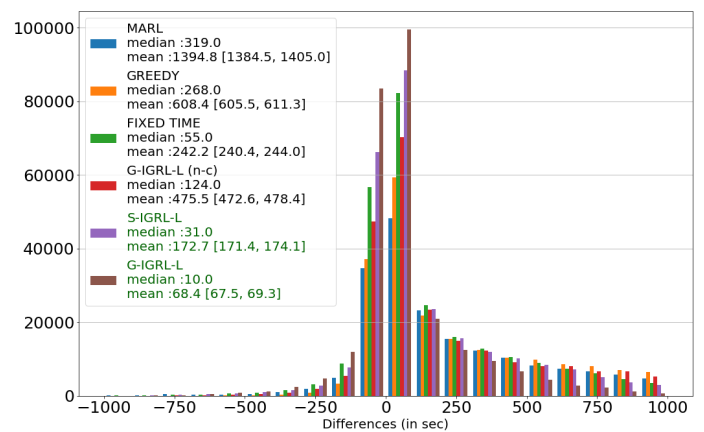


Fig. 8. Differences of Paired Trips Durations (compared to G-IG-RL-V) : **Heavy** Traffic Regime — Synthetic Road Networks

IG-RL-L. Their performances are similar in the default regime but G-IG-RL-L outperforms S-IG-RL-L in the heavy regime. This shows that G-IG-RL enables the efficient learning of transferable patterns, and that learning from a variety of road-networks is key to enable generalization to new traffic regimes. This result further emphasizes the limits of training any policy, whether it is a single policy in the context of centralized RL or multiple policies in the context of MARL, on a single road architecture. (Recall that allowing for modelling different sets of train and test networks is one of our key contributions.)

IG-RL-V is the best performing method. It has 1) the lowest trips durations, 2) the slowest congestion increase, and 3) the fastest recovery. In addition, distributions of the differences of trip-durations, paired between every method and G-IG-RL-V (Figures 7 and 8) show that a large majority of trips are completed faster using the latter method. In the default traffic regime some trips are delayed by up to a thousand seconds when using MARL or Fixed-Time instead of IG-RL-V. On the other hand, none of them are slowed down by more than a hundred seconds using IG-RL-V compared to MARL or Fixed-Time. In the heavy traffic regime, we make similar observations, with larger durations and delays. This shows that in addition to improving average performance, the



best performing method tend to distribute delays in a more equitable way.

G-IG-RL-V outperforming other methods in both traffic regimes highlights the flexibility of the GCN to exploit a finer level of granularity (i.e., data sensed at the vehicle level). However, G-IG-RL-L and S-IG-RL-L being the second bests (ex-aequo) performing methods in the default traffic regime, and G-IG-RL-L being the second best performing method when generalizing to a heavier traffic regime, we can conclude that IG-RL can also perform well with demand sensed at the lane level. As the comparison between S-IG-RL-V and G-IG-RL-V lead to the same conclusion as the one between S-IG-RL-L and G-IG-RL-L, we did not include S-IG-RL-V in this paper to avoid redundancy and improve readability.

As shown by G-IG-RL-L(n-c), removing action-correction has an important negative impact on performance and generalization to heavy traffic regime, with trips lasting longer, congestion increasing faster, and recovering slower than every other IG-RL based method.

Even though the additions described in § IV-C help MARL-IQL during training, this method ends up being the worst performing model in the current evaluation. The ranking of the learnt methods, in terms of performance, does not differ in a significant way between training and test, but MARL-IQL’s performance is much closer to the other models during training than it is during test. This suggests that policies learnt by MARL-IQL do not generalize well to new demand, even when evaluated on the traffic regime used during training. As described in § III, we hypothesize that training a policy on a variety of MDPs, which is made possible by IG-RL, prevents overfitting. Variety marginalizes out the traffic distribution experienced during training, and the particular behaviors of a set of neighbor agents corresponding to a single MDP. To a certain extent, we think that this frees this particular version of DEC-RL from the curse of non-stationarity which makes the training unstable for MARL-based methods.

### E. Experiment 2: Transfer and Scaling

1) *Description:* In this experiment the target network is Manhattan, which involves 3,971 TSCs, some complex intersections being managed by several TSCs, and 55,641 lanes. This network provides an testbed for evaluating the generalization and scaling properties of G-IG-RL approaches.

Training MARL based methods on that many intersections would imply massive time (running the corresponding simulations) and memory (storing and training one model per intersection) resources. Training S-IG-RL would enable the use of a constant number of parameters, but gathering the amount of experience required for RL on such a large road-network would not be possible in a reasonable time with the simulator and computational resources that we use. Since it can leverage zero-shot transfer (i.e. no additional training) and keep the number of parameters constant, G-IG-RL, which is trained on a set of small networks as described earlier, is the only learnt method usable in this large-scale context.

For a given road network, G-IG-RL-L requires fixed computational time, while both the computational time and memory

requirements of G-IG-RL-V increase linearly with the number of vehicles in the network. Considering the size of the experiment, even though we expect G-IG-RL-V to perform better than G-IG-RL-L considering the results of the previous experiment, we only evaluate the latter.

Evaluating methods on this large network is much more demanding than in Experiment 1. Every method is only evaluated on 5 instances of randomly generated traffic for a fixed duration of one hour and run on a single traffic regime which introduces a vehicle every second in the network. Compared with what G-IG-RL experienced during training, and what was evaluated in Experiment 1, adding a vehicle every second in a network as large as Manhattan leads to light traffic density which increases in certain areas as vehicles enter the network following asymmetric distributions based on a given random seed. Waiting for all trips to end would mean prolonging the duration of some simulations in an unreasonable way, considering that some trips might require a lot of time to be completed in such a network. Again, for computational concerns, we stop the simulation after an hour. We can therefore report aggregated results, but trips cannot be compared via pairing, as done in Experiment 1, without introducing bias.

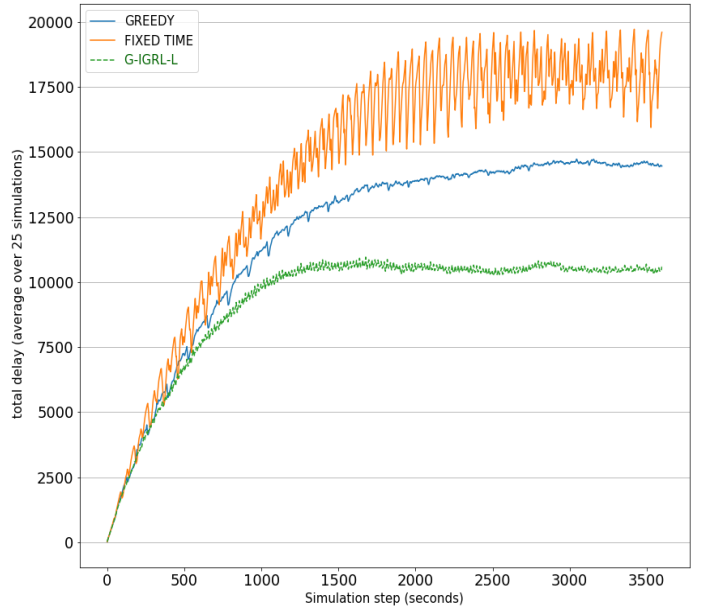


Fig. 9. Total Delay Evolution: **Light** Traffic Regime — Manhattan Island. As all simulations are running on the same road network, and the fixed time controls of many intersections are synchronized, the local delays are highly correlated across intersections and across simulations under this method, hence the periodic pattern.

2) *Results:* A first result, is the bare fact that using G-IG-RL-L, the 3,971 traffic signal controllers are operable, using a single GPU, and a model involving only 11,076 parameters. In addition, we can see that the total instantaneous delay, measured at every timestep and reported in Figure 9, shows that G-IG-RL outperforms baselines which can scale to Manhattan, in terms of the slowest congestion increase and the lowest congestion-level steady-state. Furthermore, it confirms the ability of IG-RL to generalize to different (here

lighter) traffic regime than experienced in training. These results demonstrate that using synthetic randomly generated road networks for training is a viable and efficient way to learn policies that can transfer well to real-road networks. This evaluation setting is similar in spirit to what is done in sim2real for robotics [28], [29].

## V. CONCLUSION

We introduce IG-RL, a reinforcement-learning trained method that leverages the flexible computational graphs of GCNs and their inductive capabilities [10] to obtain a single set of parameters applicable to the control of a variety of road networks. Experiments demonstrate that a training using small-synthetic networks is enough to learn generalizable patterns, which in turn enables zero-shot transfer to new road networks, as well as new traffic distributions and regimes. Experiments demonstrate that IG-RL outperforms MARL-IQL with deep neural networks, as well as both dynamic heuristic-based and fixed-time baselines. Further, generalizability over architectures, which emerges from a generalist IG-RL (G-IG-RL), helps further improve performance and generalization to new regimes of traffic. In addition, we showed that the flexibility of GCNs enables a flexible representation of the road network. Demand and structure can be represented and exploited in various ways, at their finest level of granularity, no matter the evolution of the number of entities and their respective locations in the road network.

a) *Future work:* IG-RL opens a path for the following future works: 1) The flexibility of GCNs could be key to the optimization of multi-modal transportation. We represent vehicles as nodes in IG-RL-V and we could experiment with pedestrian nodes, cyclist nodes, and many more, to ensure that traffic signal control accounts for all road-users instead of prioritizing cars. 2) In this work, the reward function used for every MDP focuses on local queues (see Equation 1). In such a setting, coordination between MDPs is limited, and a shallow GCN is able to perform well since local information is sufficient. Evaluating whether the use additional coordination mechanisms can further improve global performance could be an interesting avenue for future work. One way of addressing coordination, in the context of more global reward functions, would be to perform message passing on longer network distances by adding more layers to the GCN, or by adding recurrent mechanisms to it as done in [34].

## REFERENCES

- [1] M. Barth and K. Boriboonsomsin, "Real-world carbon dioxide impacts of traffic congestion," *Transportation Research Record*, vol. 2058, no. 1, pp. 163–171, 2008.
- [2] T. Chu, J. Wang, L. Codecà, and Z. Li, "Multi-agent deep reinforcement learning for large-scale traffic signal control," *IEEE Transactions on Intelligent Transportation Systems*, 2019.
- [3] P. Mannion, J. Duggan, and E. Howley, "Parallel reinforcement learning for traffic signal control," *Procedia Computer Science*, vol. 52, pp. 956–961, 2015.
- [4] W. Genders and S. Razavi, "Using a deep reinforcement learning agent for traffic signal control," *arXiv preprint arXiv:1611.01142*, 2016.
- [5] L. Prashanth and S. Bhatnagar, "Reinforcement learning with function approximation for traffic signal control," *IEEE Transactions on Intelligent Transportation Systems*, vol. 12, no. 2, pp. 412–421, 2010.

- [6] B. Bakker, S. Whiteson, L. Kester, and F. C. Groen, "Traffic light control by multiagent reinforcement learning systems," in *Interactive Collaborative Information Systems*. Springer, 2010, pp. 475–510.
- [7] P. Mannion, J. Duggan, and E. Howley, "An experimental review of reinforcement learning algorithms for adaptive traffic signal control," in *Autonomic Road Transport Support Systems*. Springer, 2016, pp. 47–66.
- [8] X. Wang, L. Ke, Z. Qiao, and X. Chai, "Large-scale traffic signal control using a novel multi-agent reinforcement learning," *arXiv preprint arXiv:1908.03761*, 2019.
- [9] L. Kuyer, S. Whiteson, B. Bakker, and N. Vlassis, "Multiagent reinforcement learning for urban traffic control using coordination graphs," in *Joint European Conference on Machine Learning and Knowledge Discovery in Databases*. Springer, 2008, pp. 656–671.
- [10] W. Hamilton, Z. Ying, and J. Leskovec, "Inductive representation learning on large graphs," in *Advances in Neural Information Processing Systems*, 2017, pp. 1024–1034.
- [11] C. Szepesvári, "Algorithms for reinforcement learning," *Synthesis lectures on artificial intelligence and machine learning*, vol. 4, no. 1, pp. 1–103, 2010.
- [12] H. Wei, N. Xu, H. Zhang, G. Zheng, X. Zang, C. Chen, W. Zhang, Y. Zhu, K. Xu, and Z. Li, "Colight: Learning network-level cooperation for traffic signal control," in *Proceedings of the 28th ACM International Conference on Information and Knowledge Management*, 2019, pp. 1913–1922.
- [13] Y. Wang, T. Xu, X. Niu, C. Tan, E. Chen, and H. Xiong, "STMARL: A spatio-temporal multi-agent reinforcement learning approach for traffic light control," *arXiv preprint arXiv:1908.10577*, 2019.
- [14] G. Papoudakis, F. Christianos, A. Rahman, and S. V. Albrecht, "Dealing with non-stationarity in multi-agent deep reinforcement learning," *arXiv preprint arXiv:1906.04737*, 2019.
- [15] S. Omidshafiei, J. Papis, C. Amato, J. P. How, and J. Vian, "Deep decentralized multi-task multi-agent reinforcement learning under partial observability," in *Proceedings of the 34th International Conference on Machine Learning-Volume 70*. JMLR. org, 2017, pp. 2681–2690.
- [16] R. S. Sutton and A. G. Barto, *Reinforcement Learning: An Introduction*, 2nd ed. The MIT Press, 2018. [Online]. Available: <http://incompleteideas.net/book/the-book-2nd.html>
- [17] S. S. Gu, T. Lillicrap, R. E. Turner, Z. Ghahramani, B. Schölkopf, and S. Levine, "Interpolated policy gradient: Merging on-policy and off-policy gradient estimation for deep reinforcement learning," in *Advances in neural information processing systems*, 2017, pp. 3846–3855.
- [18] C. J. Watkins and P. Dayan, "Q-learning," *Machine learning*, vol. 8, no. 3-4, pp. 279–292, 1992.
- [19] R. Bellman, "A markovian decision process," *Journal of mathematics and mechanics*, pp. 679–684, 1957.
- [20] H. V. Hasselt, "Double Q-learning," in *Advances in Neural Information Processing Systems*, 2010, pp. 2613–2621.
- [21] Z. Wang, T. Schaul, M. Hessel, H. Van Hasselt, M. Lanctot, and N. De Freitas, "Dueling network architectures for deep reinforcement learning," *arXiv preprint arXiv:1511.06581*, 2015.
- [22] M. Fortunato, M. G. Azar, B. Piot, J. Menick, I. Osband, A. Graves, V. Mnih, R. Munos, D. Hassabis, O. Pietquin *et al.*, "Noisy networks for exploration," *arXiv preprint arXiv:1704.10295*, 2017.
- [23] L. Busoniu, B. De Schutter, and R. Babuska, "Decentralized reinforcement learning control of a robotic manipulator," in *2006 9th International Conference on Control, Automation, Robotics and Vision*. IEEE, 2006, pp. 1–6.
- [24] T. N. Kipf and M. Welling, "Semi-supervised classification with graph convolutional networks," *arXiv preprint arXiv:1609.02907*, 2016.
- [25] M. Schlichtkrull, T. N. Kipf, P. Bloem, R. Van Den Berg, I. Titov, and M. Welling, "Modeling relational data with graph convolutional networks," in *European Semantic Web Conference*. Springer, 2018, pp. 593–607.
- [26] M. Aslani, M. S. Mesgari, and M. Wiering, "Adaptive traffic signal control with actor-critic methods in a real-world traffic network with different traffic disruption events," *Transportation Research Part C: Emerging Technologies*, vol. 85, pp. 732–752, 2017.
- [27] M. Fortunato, C. Blundell, and O. Vinyals, "Bayesian recurrent neural networks," *arXiv preprint arXiv:1704.02798*, 2017.
- [28] F. Sadeghi, A. Toshev, E. Jang, and S. Levine, "Sim2real viewpoint invariant visual servoing by recurrent control," in *Proceedings of the IEEE Conference on Computer Vision and Pattern Recognition*, 2018, pp. 4691–4699.
- [29] I. Akkaya, M. Andrychowicz, M. Chociej, M. Litwin, B. McGrew, A. Petron, A. Paino, M. Plappert, G. Powell, R. Ribas *et al.*, "Solving rubik's cube with a robot hand," *arXiv preprint arXiv:1910.07113*, 2019.

- [30] P. A. Lopez, M. Behrisch, L. Bieker-Walz, J. Erdmann, Y.-P. Flötteröd, R. Hilbrich, L. Lücken, J. Rummel, P. Wagner, and E. Wießner, “Microscopic traffic simulation using sumo,” in *The 21st IEEE International Conference on Intelligent Transportation Systems*. IEEE, 2018. [Online]. Available: (<https://elib.dlr.de/124092/>)
- [31] J. Oh, S. Singh, H. Lee, and P. Kohli, “Zero-shot task generalization with multi-task deep reinforcement learning,” in *Proceedings of the 34th International Conference on Machine Learning-Volume 70*. JMLR. org, 2017, pp. 2661–2670.
- [32] I. Higgins, A. Pal, A. Rusu, L. Matthey, C. Burgess, A. Pritzel, M. Botvinick, C. Blundell, and A. Lerchner, “Darla: Improving zero-shot transfer in reinforcement learning,” in *Proceedings of the 34th International Conference on Machine Learning-Volume 70*. JMLR. org, 2017, pp. 1480–1490.
- [33] X. Liang, X. Du, G. Wang, and Z. Han, “A deep reinforcement learning network for traffic light cycle control,” *IEEE Transactions on Vehicular Technology*, vol. 68, no. 2, pp. 1243–1253, 2019.
- [34] J. Zhang, X. Shi, J. Xie, H. Ma, I. King, and D.-Y. Yeung, “Gaan: Gated attention networks for learning on large and spatiotemporal graphs,” *arXiv preprint arXiv:1803.07294*, 2018.